INDERSCIENCE PUBLISHERS
Linking academia, business and industry through research

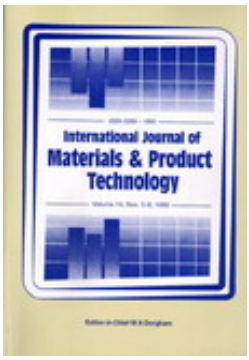

International Journal of Materials and Product Technology

ISSN online: 1741-5209 - ISSN print: 0268-1900
https://www.inderscience.com/ijmpt

Structural optimisation method of six degrees of freedom manipulator based on finite element analysis

Shudong He

DOI: 10.1504/IJMPT.2024.10062360

Article History:

Received:	20 July 2023
Last revised:	26 September 2023
Accepted:	06 November 2023
Published online:	22 February 2024

Structural optimisation method of six degrees of freedom manipulator based on finite element analysis

Shudong He

Intelligent Manufacturing and Mechanical Engineering,
Hunan Institute of Technology,
Hengyang, 421002, China
Email: heshudong.1987@163.com

Abstract: In order to improve the optimisation effect of the robotic arm structure from multiple aspects, this paper designs a six degree of freedom robotic arm structure optimisation method based on finite element analysis. Firstly, the relative motion relationship between the rotating joint and the connecting rod was established based on the D-H theory. Then, we divide the mesh elements of the robotic arm structure in ANSYS software and analyse the parameter optimisation redundancy of the robotic arm. Finally, an optimisation equation set was established, and feasible structural optimisation parameters were obtained through solving and finite element verification. The experimental results show that under different load conditions, the maximum load of the robotic arm is increased to 14 kg, the mass of the robotic arm is reduced by about 11%, and the maximum stress is reduced to 13.54 MPa. At the same time, the reachable distance of the robotic arm in three-dimensional space is significantly increased.

Keywords: six degrees of freedom mechanical arm; mechanical arm structure; D-H theory; kinematics model; ANSYS software; optimisation margin.

Reference to this paper should be made as follows: He, S. (2024) 'Structural optimisation method of six degrees of freedom manipulator based on finite element analysis', *Int. J. Materials and Product Technology*, Vol. 68, Nos. 1/2, pp.71–85.

Biographical notes: Shudong He received his PhD in Mechanical Engineering from Hunan University of Science and Technology 2022. He is currently a Lecturer majoring in Mechanical and Electrical Engineering at Intelligent Manufacturing and Mechanical Engineering, Hunan Institute of Technology. His main research interests include ocean sampling equipment and reliability.

1 Introduction

In the early days, robotic arms were mainly used in industrial production processes, which could replace simple and heavy labour activities such as human transportation to improve the efficiency of repetitive mechanical activities. With the practical application of related technologies and the mature use of related industries, the structure of the manipulator becomes more complex, and its flexibility and execution accuracy are constantly enhanced. It can not only replace human resources in industrial production operations to efficiently complete heavy or high-precision work, but also replace human

beings in military, aerospace, agricultural production management, medicine, resource mining and other fields to perform dangerous, high-intensity, high-precision work (Seghiri et al., 2023). The six degrees of freedom manipulator is one of the most widely used manipulators at present. Its joint type universal structure brings redundancy, which enables it to choose different installation methods according to the use needs. It has stronger mobility, effectively expanded workspace, and greatly improved the reliability of performing tasks (Yang et al., 2022).

At present, the optimisation of the manipulator mainly focuses on its motion trajectory, execution control and other aspects. The structural optimisation of the manipulator is mostly through the work spatial analysis and dynamic analysis of its structural movement. Relevant research theories and foundations have been applied and achieved certain results. Among them, Morales et al. (2022) take a four degree of freedom robotic arm as the research object. By analysing the dynamic response of its motion mechanism under different loads, the structural size parameters of the robotic arm are continuously adjusted with pre-set constraints to achieve structural optimisation under maximum load. After analysing the force form of the manipulator in Zhang et al. (2022), the stiffness model is constructed according to Castigliano's second theorem. Then, through periodic topology optimisation, the discrete subdomain hole shapes in the low stress region of the robotic arm are optimised, thereby achieving the global stiffness optimisation of the robotic arm under the influence of complex alternating loads. The inverse kinematics optimisation process of the manipulator is established based on the optimal joint angle parameters in Zhang et al. (2019). The method first calculates the analytical expression of the joint angle of the manipulator, and then combines the Newton iterative method and Lagrange multiplier method to transform the design process of the optimal configuration of the manipulator into the optimisation process of the optimal marker parameters. On this basis, the optimisation design of the manipulator structure is carried out from the joint configuration and joint torque. A multi-objective function-based optimisation method for the design of mechanical arm structural parameters is proposed in Zhao et al. (2022). In order to overcome the difficulties in mathematical description of the workspace, load capacity and speed of the two arms of the end effector of a manipulator, the optimisation objective function was established by using the triple integration method and the operability function, respectively, and the coupling relationship between the three optimisation objectives was determined by using the coupling analysis method. Then, the fuzzy analytic hierarchy process is used to linearly weight multiple optimisation functions according to the index weight to obtain the comprehensive multi-objective optimisation function. Then, the optimal value of the objective function is solved based on the particle swarm optimisation algorithm to obtain the structural parameters of the dual arm, so as to optimise the comprehensive performance of the dual arm robot.

However, in practical application, it is found that when the above methods are applied to the structural control of a six degrees of freedom manipulator, the optimised boom displacement is large, which not only exceeds the effective working range of the boom but also increases the mass of the manipulator boom, limiting the operating range and flexibility of the manipulator execution end, and the structural optimisation effect has certain application limitations. In response to this issue, this article proposes a six degree of freedom robotic arm structure optimisation method based on finite element analysis, aiming to improve the optimisation effect of the robotic arm structure from multiple perspectives. The innovative technology route is as follows:

1 Establish relative motion relationship based on D-H theory: firstly, use D-H theory to establish accurate relative motion relationship between the rotating joint of the robotic arm and the connecting rod. This ensures that the model has the correct constraints and degrees of freedom.

2 Finite element analysis and mesh generation: use ANSYS software to conduct finite element analysis of the robotic arm structure and generate appropriate mesh elements. By accurately meshing, the performance and characteristics of the robotic arm can be more accurately evaluated.

3 Parameter optimisation margin analysis: conduct optimisation margin analysis on the parameters of the robotic arm. By determining the optimisation space and range of parameters, the optimal parameter combination can be found and the performance of the robotic arm can be improved.

4 Establishing an optimisation equation set: based on the design requirements and objectives of the robotic arm, a corresponding optimisation equation set was established. These equations describe the constraints and objective functions that need to be met, laying the foundation for subsequent optimisation processes.

5 Solution and finite element verification: by solving the optimisation equation system, feasible parameters for structural optimisation were obtained. Next, finite element analysis is used to validate the optimisation results to ensure that the design requirements and performance indicators are met.

The experimental results show that under different load conditions, using this innovative method, the maximum load of the robotic arm is increased to 14 kg, the mass is reduced by about 11%, the maximum stress can be reduced to 13.54 MPa, and a significant increase in the achievable distance for three-dimensional space operations is achieved. This proves that the innovative technology route has effectively improved the optimisation effect of the robotic arm structure.

2 Structural optimisation of six degrees of freedom manipulator

The six degree of freedom robotic arm model established in this article has advantages such as comprehensive consideration of degrees of freedom, high flexibility, precise modelling, multi physical field coupling analysis, and reliability verification. This model can simultaneously consider the translational and rotational degrees of freedom of the robotic arm, adapt to different working conditions and task requirements, and provide accurate analysis results through accurate modelling and material nonlinearity considerations. In addition, the model can consider various physical field coupling problems and verify its reliability through finite element analysis. In summary, the six degrees of freedom robotic arm model established in this article provides effective tools and methods for the optimisation and performance evaluation of robotic arm structures.

2.1 Kinematics analysis of robot arm

When analysing the model of a six degrees of freedom robotic arm based on finite element analysis, it has rationality and characteristics. In terms of rationality, finite element analysis can accurately model the various components of the robotic arm, taking into account factors such as material nonlinearity, geometric nonlinearity, and contact, providing accurate analysis results. At the same time, this analysis model can consider various physical field coupling problems generated by the robotic arm during motion, such as structural deformation, heat conduction, and fluid flow, and comprehensively evaluate the performance and response of the robotic arm. In terms of characteristics, this model can handle multi degree of freedom robotic arms, including translation and rotation, to comprehensively evaluate their performance and stability. In addition, the high flexibility of the finite element analysis model can be analysed for different loads and working environments, and can adapt to different task requirements through rapid iteration and optimisation. In summary, the six degree of freedom robotic arm analysis model based on finite element analysis has rationality and characteristics, which can accurately evaluate the performance of the robotic arm and meet diverse needs. Each joint of the manipulator is connected with different types of connecting rods. To facilitate the use of finite element analysis software to analyse the structural mechanics performance of the six degrees of freedom manipulator, the kinematics model of the manipulator in the workspace is analysed. For a six degrees of freedom manipulator, the articulated link can rotate, translate and other movements, and it has three degrees of freedom of rotation and three degrees of freedom of translation in the three-dimensional coordinate system of the workspace (Wei et al., 2023). Calculate the degree of freedom Z of a robotic arm in motion according to the following equation:

$$Z = 3M - 2P_G - 2P_D \tag{1}$$

In the formula, M represents the number of active components when the robotic arm executes corresponding work instructions; P_G and P_D represent the number of high and low pairs of different connections in the rigid link, respectively.

For a rigid link, its displacement in the plane and rotation in space can be represented by three displacement vectors and three pose vectors, respectively, to establish the coordinate vector conversion relationship between the link in the fixed spatial coordinate system O and the rigid body coordinate system o (Shubh et al., 2023).

According to the principles of spatial geometry, the non-homogeneous composite transformation between two fixed spatial coordinate systems O and the rigid body coordinate system o can be obtained. Orthogonal transformation is performed to obtain the following homogeneous transformation form of the spatial coordinate system:

$$\begin{bmatrix} P^O \\ 1 \end{bmatrix} = \begin{bmatrix} R_o^O & O_{R^o} \\ 0 & 1 \end{bmatrix} \begin{bmatrix} P^o \\ 1 \end{bmatrix} \tag{2}$$

In the above equation, P^O and P^o respectively represent the position coordinates of a point p on the rigid link in the corresponding fixed spatial coordinate systems O and o rigid body coordinate systems; R_o^O represents the orthogonal rotation matrix, which means the vector change relationship between the point in the fixed spatial coordinate system O and

the rigid coordinate system; O_{R^o} represents a homogeneous vector matrix of the rotation matrix.

Establish a vector change relationship description matrix between the fixed spatial coordinate system and each connecting rod spatial coordinate system in sequence according to the above process. According to the D-H theory, the linkage used by a robotic arm to perform tasks can be described using four parameters. The relationship between the mathematical coordinate systems of the two joints on the linkage is shown in Figure 1.

Figure 1 Schematic diagram of the D-H coordinate system of the robotic arm

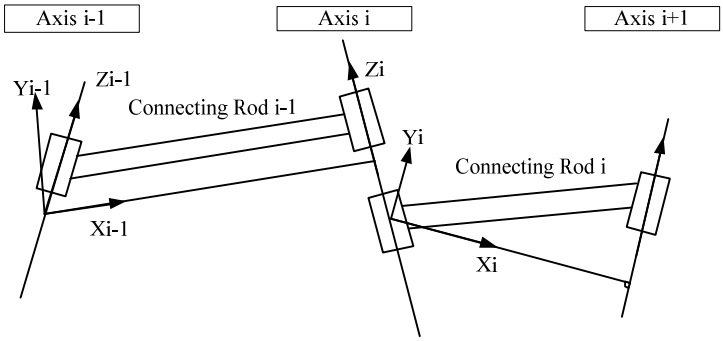

The steps to establish the D-H coordinate system of the six degrees of freedom manipulator joint are as follows:

Step 1 Using the joint base as the numbering order, the axis l_1 of the joint G_1 and its coordinate axis z are combined to point upwards in the specified direction. The connecting rod l_1 connected to the joint G_1 coincides and remains perpendicular to the z-axis of the joint G_1, with the x-axis direction pointing from G_1 to G_2. According to the right-hand rule, the y-axis of the joint G_1 is specified.

Step 2 By analogy, the coordinate system of each joint G_i of the six degrees of freedom manipulator is established, and the joint parameters under the D-H theory are obtained: the length ZD_i of the connecting rod adjacent to the joint, the torsion angle θ_i of the connecting rod operation, the joint displacement deviation XD_i, and the joint rotation angle γ_i.

Step 3 Based on the relative position transformation relationship between coordinate systems, the pose expression of the joint G_i relative to the coordinate system of the joint G_{i+1} can be obtained:

$$ {}^{i-1}_{i}T = R_{xi-1}\left(ZD_{i-1}, \theta_i\right) T_{xi-1}\left(ZD_{i-1}, XD_i\right) R_{xi-1}\left(XD_{i-1}, \gamma_i\right) \tag{3} $$

In the above equation, R is the rotation relationship matrix between two coordinate systems; T is the translation relationship matrix between two coordinate systems. According to the D-H coordinate system, the relative positional constraints of different robotic arm components during operation can be determined (Liu et al., 2023). The analysis model of the manipulator is

established in the finite element model, and the force of the manipulator is analysed to obtain the structural optimisation parameters.

2.2 Structural dynamic balance equations for finite element analysis

When the six degrees of freedom manipulator moves, each link is connected in series, and the pose transformation matrix between the two links is multiplied in turn to obtain the pose coordinate system of the manipulator end setting mechanism in the following formula, thus establishing the motion model of the manipulator (Gao et al., 2023):

$$T = 1_T 2_T 3_T 4_T 5_T 6_T \tag{4}$$

According to the above equation, once the pose vector of the executing component at the end of the robotic arm is known, the motion model can be inverted to obtain the inverse motion solution of the robotic arm. Due to the limitation of the structural motion of the manipulator and the rotation angle of the joint, the inverse solution of the equations of motion has a unique or few common understandings. The range of the structural parameters of the manipulator corresponding to the reasonable solution is the range of parameters that can be optimised and adjusted.

This study uses ANSYS finite element analysis software to perform mechanical analysis on the optimised robotic arm structure. First, scan the global mesh of the six degrees of freedom manipulator to control the boundary constraints of the simplified manipulator model (Sun et al., 2021). Considering the conventional dimensions and geometric properties of the structural components of the robotic arm, a tetrahedral mesh form is selected to divide the component structure. After setting the correlation parameter 5.8, smoothness parameter 12, and mesh transition parameter 1.5, local mesh refinement was performed on the joint connecting rod connections and other positions, resulting in 2478562 finite element elements.

In the software, the elastic modulus of the material of the mechanical arm is defined as 70 GPa, the Poisson's ratio is 0.42, the average value of 2.85 g/cm^3 of the material density of each structural member is taken, and the maximum tensile stress of the member is 300 MPa. Combined with the stress parameters of the whole machine material, the maximum allowable stress of the finite element analysis is 135 MPa, and the structural factor of safety is 2.2.

The finite element processing software divides the mechanical arm's load-bearing structure into several nodes connected to elements, and the stress within the elements is superimposed to obtain the stress of the corresponding component (Cheng, 2021).

The stiffness equation of the component element after finite element separation is as follows (Li et al., 2019):

$$[F] = [Q][W] \tag{5}$$

In the above equation, $[F]$ represents the external force received by the robotic arm component; $[Q]$ refers to the finite element stiffness matrix of the overall structure of the manipulator component; $[W]$ is the finite element node displacement matrix of the overall structure of the component. According to the diagram in Figure 2, apply load to the six degrees of freedom manipulator as a whole, and conduct structural finite element discrete analysis.

Figure 2 Overall load constraints of the robotic arm

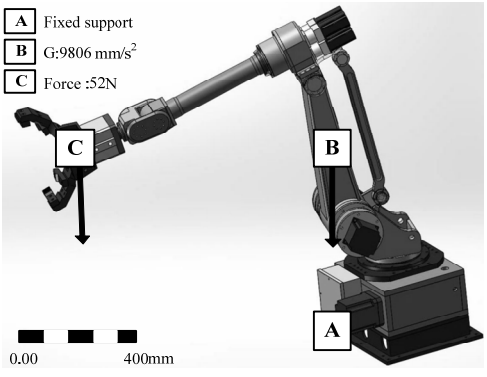

The mechanical arm is subjected to force, and the acceleration of structural vibration can be ignored, resulting in inertial loads that have little impact on structural stability. In finite element analysis, the construction quality distribution of each component of the robotic arm structure is uniform. After applying the overall load constraint, the structural dynamic balance equation of the discrete finite element is as follows (Xu et al., 2021; Dong et al., 2022):

$$[H]\{a\}+[\mu]\{v\}+[Q]\{x\}=\{F[y]\} \tag{6}$$

In the above formula, $[H]$ is the mass matrix of the manipulator structure after finite element discretisation; $[\mu]$ represents the damping matrix of discrete elements; $\{x\}$ is the displacement matrix of component element nodes; $\{a\}$ is the acceleration parameter matrix of the structural finite element method; $\{v\}$ is the velocity parameter matrix of discretisation finite element of structure. $\{F[y]\}$ represents the load parameter matrix on each connection node of the discretisation finite element y of the manipulator component.

Perform modal analysis on the structural components of the robotic arm in ANSYS, obtain the sixth order vibration mode cloud map of the structural components, and determine the natural frequency changes of the robotic arm under corresponding load constraints. By using the vibration mode change data of finite element analysis as the constraint conditions for the influence of structural stiffness and strength, the analysis and solution can determine that the strength of the boom structure meets the optimisation design space, and carry out structural optimisation design on it.

2.3 Optimise the structural parameters of the robotic arm

The basis for selecting multi-objective optimisation algorithms includes problem characteristics, algorithm performance, and algorithm adaptability. However, multi-objective optimisation faces nonlinear and high-dimensional problems, as well as potential conflicts between objectives and challenges at the forefront of Pareto. To avoid the algorithm falling into local minima, multiple strategies can be adopted. Firstly, consider using a combination of multiple algorithms to integrate different search strategies to improve global search capabilities. Secondly, by attempting multiple initial points to run the optimisation algorithm, the chances of discovering the global optimal solution are increased. In addition, methods such as limiting search space and combining

iterative optimisation with local search are also effective. Therefore, by comprehensively utilising appropriate algorithm selection and multiple strategies, the effectiveness of multi-objective optimisation can be improved and local minima can be avoided. The above finite element analysis results of the six degrees of freedom manipulator are taken as the basis and parameter limits for the optimisation of the manipulator structure parameters. Combining the dynamic and static mechanical analysis results of the manipulator, the optimisation model of the manipulator structure is established. Utilise parameter optimisation calculation results to obtain the optimal structural parameters under finite element analysis constraints.

The main factors that affect the motion sensitivity of a robotic arm include the volume of the robotic arm, the thickness of the structural material, and the size of the boss at the joint connection. Among them, the mechanical arm structure is simplified into a hollow rod structure to reduce the self weight of the mechanical arm, while reserving space for optimising the thickness of the structural material. In the finite element analysis software, the floating range for the volume of the main body of the robotic arm and the thickness of the structural material is set to ±5%, and the optimised floating range for the size of the convex boss at the joint connection is set to ±2.5% (Wang, 2021). Taking the above three influencing factors as the optimisation objective, the optimisation equation of six degrees of freedom manipulator structure is established. Due to simplifying the structure of the robotic arm into a hollow rod, the volume of the robotic arm is related to the thickness of the structural material. Therefore, an optimisation objective is established as shown in the following equation (Chen et al., 2021; Shao et al., 2019):

$$\min\left(V_d, V_s\right) \tag{7}$$

Among them,

$$V_d = \pi\left(R_w^d - R_n^d\right)^2 L_d \tag{8}$$

$$V_s = \pi\left(R_w^s - R_n^s\right)^2 L_s \tag{9}$$

In the above formula, V_d and V_s represent the volume of the robotic arm's upper arm and lower arm, respectively; R_w and R_d represent the inner and outer diameters of the hollow rods of the upper and lower arms, respectively, with the corresponding lower corner markers indicating the distinction between the upper and lower arms; L represents the length of the corresponding mechanical arm structural component. Half of the difference in inner and outer diameters of the hollow rod is the thickness of the mechanical arm structural material (Antonov et al., 2022). Taking structural parameters as the optimisation objective and ensuring the practical applicability of the structure itself, the following maximisation of stiffness is introduced as another optimisation objective:

$$\min E(c) = F^T X \tag{10}$$

In the above equation, $E(c)$ represents the deformation energy generated by the structural components of the robotic arm under external loads; F is the load vector of the structure; X is the structural displacement vector. The combination of formulas (7) and (10) constitutes a multi-objective optimisation function for the mechanical arm structure, with the following constraints:

$$\begin{cases} 0.09 \le R_w^d \le 0.13 \\ 0.05 \le R_n^d \le 0.08 \\ 0.07 \le R_w^s \le 0.11 \\ 0.04 \le R_n^s \le 0.07 \\ 0.65 \le L_d \le 0.85 \\ 0.50 \le L_s \le 0.70 \\ f = \dfrac{V_s + V_d}{V_0} \\ 0 < \rho_{\min} \le \rho_i \le \rho_{\max} \end{cases} \tag{11}$$

In the above equation, f represents the proportion of materials in the optimised and adjusted part of the structure when optimising the structure; V_0 represents the volume of space that the robotic arm can optimise; ρ_i represents the element relative density of discretisation finite element i of the structure; $\rho_{\min}$ and $\rho_{\max}$ represent the lower and upper limits of unit relative density, respectively, and their values are determined by the material properties of the robotic arm components (Wang et al., 2021). Solve the multi-objective optimisation equation, combine with the specified value range of the boss size at the joint connection, obtain several groups of optimised adjustment parameters, input the adjusted parameters into the finite element model of the six degrees of freedom manipulator, and impose constraints. The factor of safety of the optimised structure is higher than the set value, and the mechanical arm after structural parameter adjustment can effectively reduce the structural mass within the constraint range, and the relevant parameters are improved compared with those before optimisation.

3 Experimentation

In order to verify the practical application performance of the six degrees of freedom manipulator structure optimisation method based on finite element analysis designed above, the following experimental process is designed.

3.1 Experimental design

At the beginning of the experiment, the six degrees of freedom manipulator with a known parameter is selected as the experimental object. The main technical parameters of the manipulator entity are shown in Table 1.

Input the parameters of the robotic arm into the software, set the load data of the robotic arm under different working conditions, and obtain the main structure and related working parameters of the unoptimised front robotic arm, which are imported into the software ADASM. Based on the relative motion relationships between the main components of the robotic arm during actual operation, establish motion constraints and torque constraints for the robotic arm model components in ADASM to ensure that the virtual prototype can move as a whole during simulation.

Table 1 Main technical parameters of experimental robotic arm

Project	*Parameter*	*Range of value fluctuation*
Number of control axes	6	-
Load	10 kg	±20%
Overall quality	100 kg	-
Mass of manipulator	48 kg	-
Operating voltage	220-V rated voltage	±10 V
Control voltage	24 V	±5%

In order to obtain a more intuitive optimisation effect on the experimental robotic arm structure, the robotic arm structure optimisation method mentioned in Zhang et al. (2019, 2022) is introduced as a comparative method. Determine the specific range of optimisation parameters for the robotic arm structure using the relevant constraints in ADASM, and obtain the specific optimisation parameters using three methods. Adjust the parameters of the experimental prototype according to the optimisation parameters of each optimisation method to obtain the optimised mechanical arm prototype. Install a displacement sensor on the main arm of the robotic arm to collect the basic parameters of the prototype during movement. The experiment selects the motion space range of the main arm of the robotic arm optimised by different methods as a comparative indicator, and analyses and compares the actual effects of various structural optimisation methods.

3.2 Optimise experimental results and analysis

Based on the basic parameters of the experimental prototype, set the operating load of the robotic arm to 10 kg, 12 kg, and 14 kg, and compare the rotation angle of the main arm joint of the virtual prototype of the robotic arm before and after the optimisation method in this paper. The experimental data is shown in Figure 3.

Figure 3 Comparison of joint rotation angles before and after virtual prototype optimisation, (a) condition 1 (b) condition 2 (c) condition 3

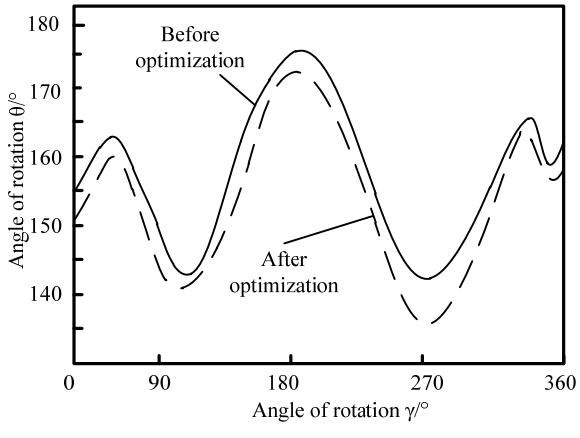

(a)

Figure 3 Comparison of joint rotation angles before and after virtual prototype optimisation, (a) condition 1 (b) condition 2 (c) condition 3 (continued)

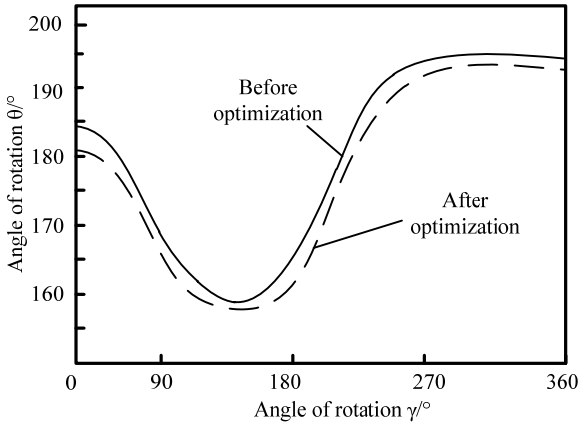

(b)

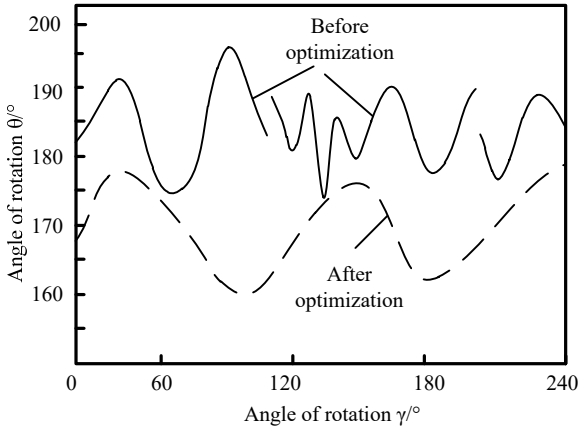

(c)

It can be seen from the analysis of Figure 3 that under the working conditions 1 and 2 with the load of 10 kg and 12 kg, respectively, the joint rotation angle curve of the virtual prototype of the mechanical arm before optimisation is smooth, but under the working condition 3 with the load of 14 kg, the joint rotation angle curve of the mechanical arm appears obvious fracture, indicating that hysteresis occurs during joint rotation. Under the three working conditions, the optimised joint rotation angle curves of the virtual prototype of the robotic arm using the method presented in this article are continuous and smooth, and the optimised angle curve is located below the curve before optimisation, with a maximum distance between the curves approaching 8°. This indicates that the optimised robotic arm structure can achieve the operation goal with a smaller rotation angle, effectively reducing the probability of joint wear under corresponding working conditions. And after the optimisation of the method in this article, the maximum load of

the robotic arm is increased to 14 kg, which increases the working adaptability range of the robotic arm.

3.3 Comparative experimental results and analysis

To further validate the application advantages of the method proposed in this paper for optimising the structure of robotic arms, the structural optimisation methods in Zhang et al. (2019, 2022) are compared. Analyse the optimised robotic arms using various methods in ADASM to obtain the maximum stress and mechanical main arm mass of the optimised virtual prototype under corresponding working conditions. The specific analysis results are shown in Table 2.

Table 2 Analysis results of virtual prototype of robotic arm

Operating order number	*Method of this paper*		*Method of Zhang et al. (2022)*		*Method of Zhang et al. (2019)*	
	Maximum stress (MPa)	*Main arm weight (kg)*	*Maximum stress (MPa)*	*Main arm weight (kg)*	*Maximum stress (MPa)*	*Main arm weight (kg)*
1	14.75	6.85	17.82	8.45	16.97	8.26
2	13.54	6.51	16.96	7.98	16.23	7.34
3	15.32	7.34	19.01	11.17	18.65	9.98

By analysing the data in Table 2, it can be seen that under the same working conditions, the maximum stress on the optimised mechanical arm structure using the method proposed in this paper is smaller than that of the optimised mechanical arm using the methods proposed in Zhang et al. (2019, 2022). And according to the material characteristics constraints of the robotic arm physical prototype, it can be seen that the optimised robotic arm structure using the Zhang et al.'s (2019) method has a certain possibility of fracture in practical applications and operating conditions, which affects the service life of the robotic arm. From the perspective of the optimised mass size of the main arm structure of the robotic arm, the optimised main arm mass of this method has decreased by about 11% compared to the prototype parameters, reducing the possibility of the optimised robotic arm being limited by the body mass during operation.

Taking condition 1 as the actual verification scenario, according to the optimisation parameters of the three methods, adjust the structural parameters of the experimental prototype of the six degrees of freedom manipulator. Set the same work instructions and measure the effective working space of the robotic arm during operation using sensors. After structural optimisation, the motion space of the robotic arm is projected on a three-dimensional coordinate plane, and the comparison results of the working space are obtained as shown in Figure 4.

By analysing the graphical information shown in Figure 4, it can be seen that under condition 1, the operational reach distance of the optimised robotic arm in three-dimensional space is higher than that of the optimised robotic arm in Zhang et al.'s (2019, 2022) methods. Among them, the optimisation effect of the reachable distance of the horizontal working space is the best, which has increased by about 38% compared to the optimisation results of the two reference methods. The optimised robotic arm in this article can support the end of the robotic arm to reach the designated working position to

the maximum extent, improving the efficiency of robotic arm operation in the working space.

Figure 4 Comparison of optimisation effects of manipulator working space

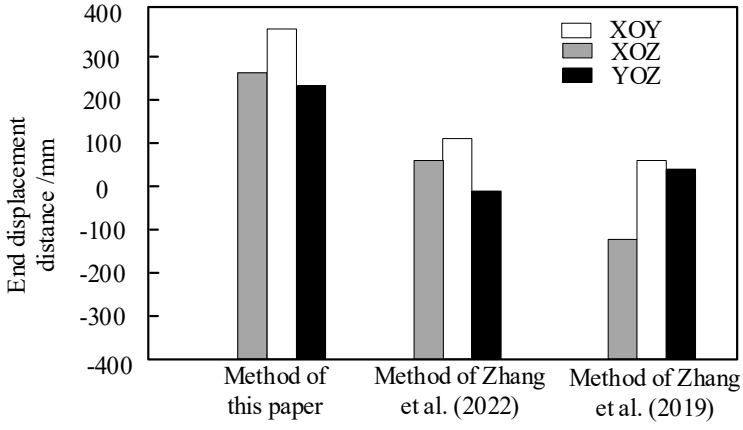

4 Conclusions

Replacing manual labour with machines to complete corresponding tasks is a necessary path for industrial development. Designing, applying, and optimising robotic arms has become an indispensable core in the future global manufacturing equipment and application management industry, and is one of the main focus points for future national development. The purpose of this study is to improve the structural optimisation effect of the six degrees of freedom manipulator, so as to increase the effective movement range of the main arm of the manipulator and reduce the mass of the overall manipulator. This paper studies the structural optimisation method of the six degrees of freedom manipulator based on finite element analysis.

After analysing the kinematics characteristics of the six degrees of freedom manipulator, the D-H theory is used to establish the relative motion relationship between the rotating joint and the connecting rod, so as to analyse the parameter optimisation margin of the manipulator. On this basis, with the adjustable margin of structural parameters as the limit, the volume, material thickness, and stiffness of the robotic arm are taken as the optimisation objectives, and an optimisation equation set is established. Through the equation set, the optimisation of the robotic arm structure is achieved.

According to the optimisation effect experiment results, after applying this method, the main arm motion range of the experimental robotic arm has been improved to varying degrees in various dimensions of operation, with the maximum effective operation range expanding by about 38%. And after structural optimisation, the overall quality of the robotic arm is reduced by about 11%, reducing the impact of its own quality on the stability of the robotic arm during operation. The above results show that the optimisation method based on finite element analysis can effectively improve the working effect of the six degrees of freedom manipulator.

References

Antonov, A., Fomin, A., Glazunov, V. and Ceccarelli, M. (2022) 'Workspace and performance analysis of a 6-DOF hexapod-type manipulator with a circular guide', *Proceedings of the Institution of Mechanical Engineers, Part C: Journal of Mechanical Engineering Science*, Vol. 236, No. 18, pp.9951–9965.

Chen, C., Chen, H., Wu, S. and Wang, J. (2021) 'Structural optimization and lightweight of industrial robot manipulator based on orthogonal test', *Machine Tool & Hydraulics*, Vol. 49, No. 5, pp.20–24.

Cheng, K. (2021) 'Kinematics and finite element analysis of the main components of robot with six degrees of freedom', *Jiangsu Science & Technology Information*, Vol. 38, No. 6, pp.44–47.

Dong, Z., Han, X., Shi, Y., Zhai, W. and Luo, S. (2022) 'Development of manipulator digital twin experimental platform based on RCP', *Electronics*, Vol. 11, No. 24, pp.4196–4196.

Gao, Y., Fang, L., Jiang, X. and Gong, Y. (2023) 'Research on tolerance optimal allocation method for a 6-DOF series manipulator based on DH-parameters', *Proceedings of the Institution of Mechanical Engineers*, Vol. 237, No. 10, pp.2291–2305.

Li, J., Qi, L. and Han, W. (2019) 'Kinematics analysis and trajectory optimization of six degree of freedom manipulator', *Journal of Changchun University of Science and Technology (Natural Science Edition)*, Vol. 42, No. 1, pp.68–73.

Liu, Y., Chen, B., Ma, L., Yang, S., Li, R. and Guo, Y. (2023) 'A novel trajectory tracking control approach for uncertain 6-DOF manipulators based on fuzzy sliding mode of radial basis function neural network', *Proceedings of the Institution of Mechanical Engineers*, Vol. 237, No. 6, pp.1032–1044.

Morales, K., Hoyos, C. and García, J.M. (2022) 'Mechanical structure design and optimization of a humanoid robot arm for education', *Journal of Autonomous Intelligence*, Vol. 5, No. 1, pp.95–109.

Seghiri, T., Ladaci, S. and Haddad, S. (2023) 'Fractional order adaptive MRAC controller design for high-accuracy position control of an industrial robot arm', *International Journal of Advanced Mechatronic Systems*, Vol. 10, No. 1, pp.8–20.

Shao, H., Lu, J., Su, Y. and You, X. (2019) 'Dynamics optimization of six-DOF articulated industrial robot', *Journal of Hefei University of Technology (Natural Science Edition)*, Vol. 42, No. 5, pp.590–594, 600.

Shubh, S., Shraddha, P., Niteesh, P., Lokhande, C., Aniket, D. and Ghorpade, R.R. (2023) 'Forward kinematic analysis of 5-DOF LYNX6 robotic arm used in robot-assisted surgery', *Materials Today: Proceedings*, Vol. 72, No. P3, pp.858–863.

Sun, Y., Xu, R. and Tian, G. (2021) 'Research on lightweight of 6-DOF manipulator based on ANSYS', *Mechanical Engineering and Automation*, Vol. 21, No. 5, pp.113–115.

Wang, S. (2021) 'Research on transient dynamics analysis of gangue selection manipulator based on ANSYS', *Coal Technology*, Vol. 40, No. 11, pp.199–201.

Wang, X., Dong, H., Lou, A., Yin, G. and Li, X. (2021) 'FEA and structural optimization on base of a mobile spraying manipulator', *Mining & Processing Equipment*, Vol. 49, No. 10, pp.50–54.

Wei, W., Liu, F., Zheng, X. and Yang, Y. (2023) 'Optimal design of heavy-duty manipulator based on RSM and NSGA-II method', *Hoisting and Conveying Machinery*, Vol. 2023, No. 2, pp.40–46.

Xu, S., Cao, X., Zhang, G., Yang, X-P. and Wang, S-J. (2021) 'Finite element analysis of hydraulic heavy mechanical arm', *Journal of Tianjin University of Technology*, Vol. 37, No. 2, pp.17–20.

Yang, X., Feng, W., Xiong, X., Wang, W. and Li, D. (2022) 'Research on structural topology and energy consumption optimization of building robot based on variable density method', *Hoisting and Transportation Machinery*, Vol. 26, No. 14, pp.40–45.

Zhang, J., Zhang, M., Li, M. and Zhang, T. (2022) 'Structural design and stiffness optimization of mechanical arm with super large telescopic ratio for ash silo cleaning', *Chinese Journal of Engineering Design*, Vol. 29, No. 4, pp.430–437.

Zhang, Y., Wang, Z., Liu, Y., Cao, B., Xie, Z. and Liu, H. (2019) 'Optimization method for the configuration of redundant manipulators', *Journal of Harbin Engineering University*, Vol. 44, No. 3, pp.329–336.

Zhao, J., Xiu, B., Wang, J. and Wan, X. (2022) 'Structural parameters design of rescue manipulator based on multi-objective optimization', *Transactions of Beijing Institute of Technology*, Vol. 42, No. 5, pp.493–501.